

Functional magnetic resonance imaging based on SEEP contrast: response function and anatomical specificity

Patrick W. Stroman^{a,*}, Jennifer Kornelsen^b, Jane Lawrence^b, Krisztina L. Malisza^{b,c}

^aDepartment of Diagnostic Radiology, Queen's University, Kingston, Ontario, Canada K7L 2V7

^bDepartment of Physiology, University of Manitoba, Winnipeg, Manitoba, Canada R3E 3J7

^cInstitute for Biodiagnostics, National Research Council of Canada, Winnipeg, Manitoba, Canada R3B 1Y6

Received 11 February 2005; accepted 7 July 2005

Abstract

Functional magnetic resonance imaging based on a non-BOLD-contrast mechanism, which we have termed “SEEP” (Signal Enhancement by Extravascular water Protons), has previously been demonstrated. Here the reproducibility of areas of activity identified with both SEEP and BOLD contrast is assessed in duplicate experiments in healthy volunteers, with relatively high resolution (1.6 mm) image data at 1.5 T. These areas of activity are equally well localized to voxels containing primarily gray matter with the two contrast mechanisms. As in previous studies, areas of SEEP activity are observed to be immediately adjacent to areas of BOLD activity, with very little overlap. The response functions were estimated for both SEEP and BOLD contrast, and are observed to be distinct. The peak SEEP response is observed to lag the BOLD response by approximately 1 s and to decay more slowly with no poststimulus undershoot. Average BOLD signal changes (GE-EPI, TE=50 ms) were observed to be $3.4 \pm 1.2\%$ (mean \pm S.D.), whereas SEEP signal changes (SE-EPI, TE=23 ms) were $1.9 \pm 0.5\%$, consistent with previous studies carried out at 0.2 and 3 T. These observations provide further support for the existence of a non-BOLD-contrast mechanism for fMRI, based on changes in extravascular spin density.

© 2005 Elsevier Inc. All rights reserved.

Keywords: fMRI; Human; Gradient echo; Spin echo; Brain; Spin density; SEEP; BOLD

1. Introduction

Functional magnetic resonance imaging based on blood oxygenation level-dependent (BOLD) relaxation time changes has become a well-established neuroimaging tool with demonstrated sensitivity to changes in neuronal activity levels [1]. However, there is evidence that physiological changes, in addition to changes in perfusion and blood oxygenation, may influence the MR signal intensity. We have previously proposed that, in addition to the BOLD effect, there is a proton-density change which can contribute to fMRI signal changes [2–5]. Functional magnetic resonance imaging data obtained in the brain and spinal cord have demonstrated that a component of the MRI signal undergoes a proton-density change of approximately 5.6%, that it has a T_2 of approximately 71 ms, an estimated T_2^* of less than 10 ms, and that it cannot be attributed to signal from blood or in-flow [2,4,5]. As a result, we have termed the effect

“SEEP” for “Signal Enhancement by Extravascular water Protons”. The areas of the brain that demonstrate SEEP signal changes during a two-hand motor task have been observed to be immediately adjacent to areas of BOLD signal change, with only slight overlap, indicating that the anatomical locations of the BOLD and SEEP mechanisms are distinct [2]. Functional magnetic resonance imaging studies employing SEEP contrast have been carried out in the brain at 0.2 and 3 T with consistent signal changes of 2% in areas of neuronal activity [2,3,6], as well as in the spinal cord at 0.2 T [6].

The properties of the signal intensity changes observed in spin-echo fMRI data have been investigated by other groups as well. Jochimsen et al. [7] employed spin-echo EPI at an echo time of 96.5 ms, as well as with a CPMG sequence with multiple refocusing pulses with an echo-planar readout at an echo time of 75 ms. Studies carried out by our group at 3 T with spin-echo EPI at an echo time of 22 ms demonstrated consistent areas of activity that were immediately adjacent to those observed with BOLD with only slight overlap [2]. Based on detailed studies of spin-echo signal changes as a function of echo time in the spinal cord at 1.5 T, we have

* Corresponding author. Tel.: +1 613 533 3245; fax: +1 613 533 6840.
E-mail address: stromanp@post.queensu.ca (P.W. Stroman).

developed a two-component model of signal changes that describes both BOLD and SEEP components [4]. Whereas fractional signal changes due to BOLD relaxation time changes increase with increasing echo time, those arising from a proton-density change appear to decrease with increasing echo time due to differences in the transverse relaxation times of the two components [4]. This model, based on experimental observations, indicates that the ratios of BOLD to SEEP signal changes [i.e., $(\Delta S/S_{\text{BOLD}})/(\Delta S/S_{\text{SEEP}})$] are 0.4, 2.1 and 3.3 at echo times of 22, 75 and 97 ms, respectively. Thus, the studies reported by Jochimsen et al. [7] and by our group [2] yielded results with significantly different sensitivities to the characteristics of signal changes observed in spin-echo fMRI data.

In a separate study at 3 T, Jochimsen et al. [8] also reported that they did not detect a proton-density change in spin-echo fMRI data, because they observed signal changes extrapolated to TE=0 that were not significantly different than zero, in contrast with our reported findings [5]. Functional magnetic resonance imaging data were acquired with spin-echo methods at four different echo times in repeated experiments (one echo time per experiment), and the voxels that were included for analysis were fixed based on active regions detected at TE=80 ms and at TE=9 ms. The average signal intensity change across the selected voxels was measured at each echo time, and this analysis therefore required the assumption that identical regions of neuronal activity are elicited in repeated experiments. Analysis of only those voxels with significant BOLD activity at TE=80 is expected to preferentially exclude the areas demonstrating SEEP signal changes and, therefore, to reveal only the BOLD effect [2]. With a spin-echo method at TE=9 ms, Jochimsen et al. [8] reported an average of 65 active voxels in the visual cortex in six volunteers, with an average signal intensity change of roughly 0.75%, at $P < 0.005$. Moreover, when all active voxels at each echo time were included in the analysis, the intercept value at TE=0 was determined to be $0.82 \pm 0.07\%$, in comparison with the value of $1.03 \pm 0.19\%$ we reported at 3 T. The findings reported by this group are thus not directly comparable with our own, but the published results to date are not inconsistent either. In contrast, other groups have reported findings that support the existence of the SEEP contrast mechanism. Luh et al. [9,10] have reported results demonstrating that signal changes in spin-echo fMRI data obtained in the brain are dominated by a proton-density change, with very little contribution from changes in transverse relaxation times. Wong et al. [6] have also demonstrated functional imaging of the spinal cord at 0.2 T using SEEP contrast [11].

The proposed mechanism of SEEP is a local increase in tissue water content arising from an altered fluid balance due to the normal production of extracellular fluid and cellular swelling. Extracellular fluid (ECF) is produced by the continuous flux of water across blood vessel walls, primarily in capillaries [12,13]. Functional imaging studies carried out with PET using radiolabelled water as a tracer have

demonstrated increased unidirectional clearance of water from the blood into the brain parenchyma at sites of neuronal activity [14,15]. This is coupled to the fact that when the neuronal firing rate increases the nerve cell body takes up more oxygen from its surroundings. A local increase in blood flow occurs, thereby providing a greater supply of oxygenated blood and a local reduction in paramagnetic deoxyhemoglobin, as well as increased perfusion pressure. This is the general sequence of events that gives rise to the BOLD signal changes related to neuronal activity [16,17]. It has been proposed that the local blood flow changes may be mediated by potassium carried by astrocytes between the active neurons and capillaries [18]. This is also linked to the swelling of neurons and glial cells at sites of neuronal activity. In the neuroscience literature, it is generally accepted that brief neuronal discharge leads to sustained swelling of adjacent glial cells [19]. Astrocytes have been shown to be depolarized during neuronal activity as a result of uptake of potassium in proportion to the number of active neurons in the vicinity and the frequency at which they fire [20]. The flux of potassium across the astrocyte plasma membrane is coupled with water transport via specific channels (aquaporins, specifically Aqp4) that are concentrated in the membranes of astrocyte end-feet facing blood vessels [21]. There is strong evidence that these channels promote the exchange of water between the brain and blood or CSF. Glutamate is also actively taken up by astrocytes and is accompanied by three Na^+ and one H^+ transported into the cell, and one K^+ transported out, with water cotransport resulting in a net flux into the cells [22]. Moreover, astrocytes are connected by gap junctions allowing passage of small molecules from cell to cell, and so they function as a continuous, large fluid volume [23].

The effects of these water fluxes are demonstrated in numerous examples in the literature. The extracellular/intracellular volume ratio has been shown to change significantly in isolated tissue samples of rat spinal cord tissue during and following neuronal stimulation. During electrical stimulation of a dorsal nerve root at 10 Hz for 1 min, the extracellular volume was observed to decrease by roughly 5% due to cellular swelling [24,25]. In another example, changes in neuronal and glial cell volumes related to neuronal activity cause changes in light transmittance and are used for imaging activity in brain slices [19,26]. Rat brain slices submerged in flowing artificial CSF solution demonstrated increased light transmittance, as a result of cell swelling, specifically at sites where electrically stimulated fibres terminated on dendrites in the hippocampus [19].

There are thus a number of physiological effects, in addition to the BOLD effect, that could potentially influence the MR signal in relation to neuronal activity. The purpose of the current study is to further investigate the proton-density change contribution to signal changes in fMRI data obtained with spin-echo methods, which we have termed “SEEP”. This is carried out by investigating the relative locations of SEEP and BOLD activity at relatively high resolution and by

estimating the response function for SEEP. This is equivalent to the hemodynamic response function for BOLD, but as yet the SEEP response has not been proven to be hemodynamic in origin. The response function (HRF) in this context is meant to indicate the linear transfer function that relates the neuronal activity-related signal intensity time course (S) to the stimulation paradigm (P) via the expression $S=P\otimes\text{HRF}$ (where \otimes signifies the convolution operation) [27]. This will enable more precise analysis of SEEP fMRI data with more stringent statistical thresholds than have previously been reasonable in the absence of an accurate model paradigm.

2. Methods

Eight healthy volunteers were studied in a 1.5-T GE Signa Horizon LX clinical MR system. Initial three-plane localizer images were acquired to provide an anatomical reference for prescribing slice positions. Functional image data were acquired from eight 4-mm-thick transverse slices, positioned parallel to the inferior points of the corpus callosum, using echo-planar imaging with a 128×256 matrix and a 20-cm field of view. In separate experiments, data were acquired with SEEP contrast (spin-echo EPI, TE=23 ms, TR=3 s, 90° flip angle) and BOLD contrast (gradient-echo EPI, TE=50 ms, TR=3 s, 90° flip angle). Activity in the motor and sensory areas was elicited by having the subject perform a two-hand finger-touching task. A block design was used with eight alternated periods of rest and finger-touching, each of 24-s duration. This stimulation paradigm was chosen to be consistent with previous studies employing SEEP contrast [2–4]. Although a brief stimulus might be assumed to be preferable for estimating the response function, event-related studies have never been carried out with SEEP contrast, and prior to this study no model was available for estimating the signal intensity time-course response to a brief stimulus in order to identify the active voxels in such an experiment. Hence, a stimulation paradigm that was known to elicit a detectable SEEP response was chosen. Functional magnetic resonance imaging experiments were carried out four times with each subject, twice with SEEP contrast and twice with BOLD contrast. Anatomical reference images were also acquired from 16 transverse slices, 4-mm thick, eight of which were coplanar with the functional image data. Reference images were acquired with a fast spin-echo method with an echo-train length of 8, a 256×256 matrix, four averages, and with T_1 weighting (TE/TR=12/500), T_2 weighting (TE/TR=87/3000) and proton-density weighting (TE/TR=12/3000).

Data were analyzed initially by means of correlation to a boxcar model paradigm after smoothing in-plane with a 3×3 boxcar filter. Correlation T maps were constructed for each experiment and were combined with a conjunction analysis by taking the minimum T value at each voxel [28]. Separate conjunction maps were made for BOLD and SEEP contrast. Time-course data from active voxels were used to determine the average response to the stimulus, which was in turn used

to estimate the response function (HRF) [29]. The response function was determined by deconvolving the observed signal intensity time course (S) with the boxcar stimulation paradigm (P) using the MatLab “deconv” function (The Mathworks, Natick, MA). The response function thus obtained was verified by performing the inverse operation of convolving it with the boxcar paradigm and comparing the result with the observed signal-intensity time course, i.e., $S=P\otimes\text{HRF}$. Data with SEEP contrast were then reanalyzed with a modified paradigm based on the observed response function in order to estimate the optimal model paradigm in an iterative fashion.

The response function that was determined in this fashion was then used as the starting point for more precise analyses of the SEEP and BOLD data. The original image data were used without spatial smoothing, but with temporal filtering to remove the high-frequency components. A general linear model approach [29,30] was used with a basis set constructed of two elements: (a) the stimulation boxcar paradigm convolved with the response function, and (b) a constant function. A statistical parametric map was then constructed for each data set using a high statistical threshold ($P<10^{-4}$) in order to detect more precisely the areas of activity with each method. The response function was then calculated from the observed average time course for each data set, and the model was adjusted to the closest approximation of all of the observations. This process was repeated until a model response function was obtained for both BOLD and SEEP data that corresponded well with all of the observed responses, and when further iterations of the process did not result in significant changes to the results.

The anatomical reference images with T_1 -, T_2 - and proton-density weighting were used to create a segmented map of gray matter, white matter, mixed gray and white matter, CSF, skull and background, for each subject. This was achieved by defining a three-dimensional vector for each voxel composed of the signal intensities in each image, divided by the average intensity in all three images, in order to provide a consistent comparison. Voxels were then repeatedly divided into groups, to create 32 groups of voxels with similar vectors. Model vectors were constructed for each tissue type based on the expected T_1 , T_2 and relative proton density for each, as well as the image acquisition parameters, and these models were then used to assign a tissue type to each group. The resulting segmented map was then used to characterize the anatomical sites of activity identified with BOLD and SEEP contrast, by computing the proportion of active voxels within each tissue type.

3. Results

Areas of signal-intensity change that were significantly correlated with the time course of rest and performance of the two-hand motor task were observed in every experiment, with both SEEP and BOLD contrast. These areas of activity were well localized to the bilateral sensory and motor areas,

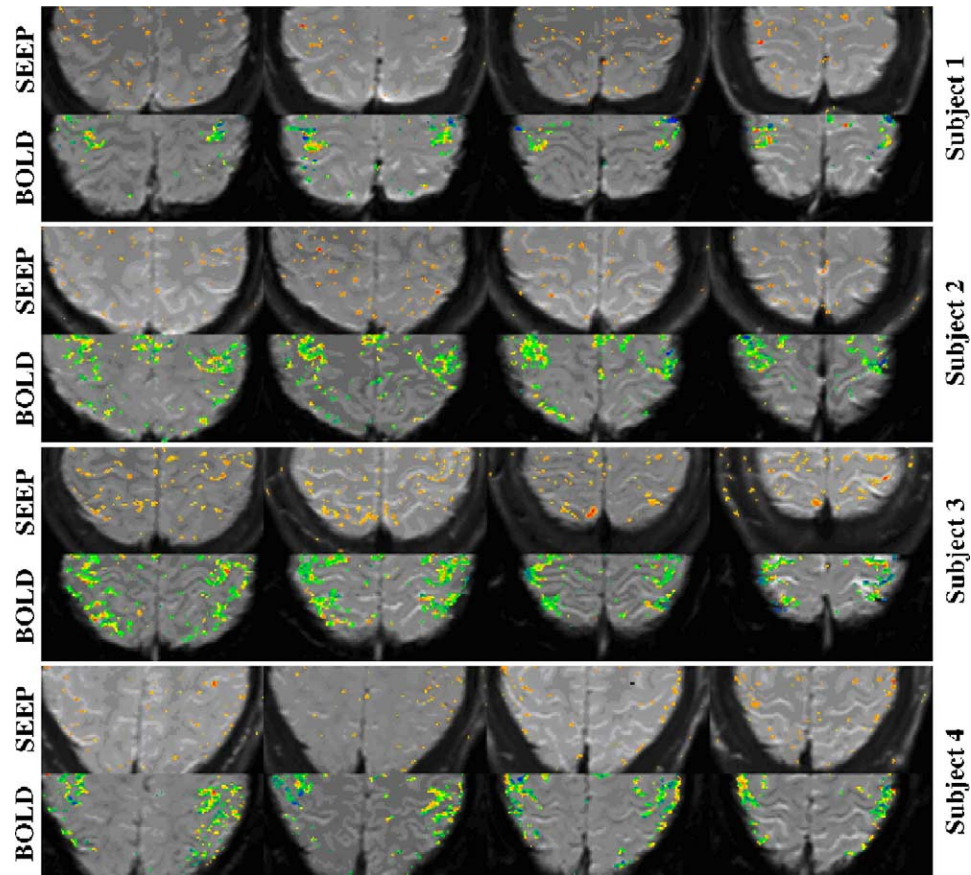


Fig. 1. Conjunction maps computed for BOLD and SEEP contrast in four representative volunteers. Maps of T values for each experiment were constructed using the correlation between a boxcar model paradigm and the intensity time course at each voxel, and conjunction maps were computed by taking the lowest T value in duplicate experiments. The results are shown with a threshold of $T \geq 2$. Each row shows the results from four selected slices in each volunteer, and results obtained with BOLD and SEEP contrast are shown in separate rows. The images are cropped to show only the posterior half of each slice, for clarity. Red indicates the highest T value in each experiment, and colors show lower values in decreasing spectral order.

and the supplementary motor area, and also appeared to be very well localized to gray matter regions. Representative conjunction maps calculated for duplicate experiments in each subject are shown in Fig. 1. These maps demonstrate the lowest T score at each voxel in duplicate experiments,

with only values of $T \geq 2$ shown, and so voxel-wise reproducibility is demonstrated as well. An initial estimate of the SEEP response function was determined from the areas of activity identified in the conjunction maps and was used for subsequent analyses.

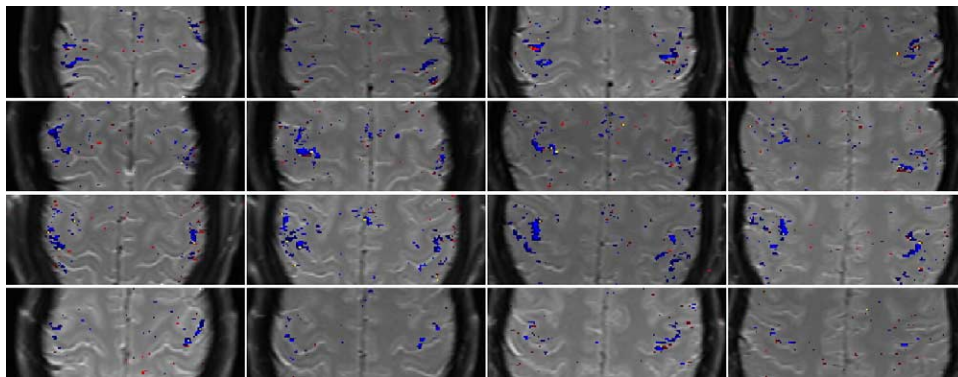


Fig. 2. Representative examples of areas of BOLD and SEEP activity identified by means of a general-linear-model method with $P \leq 10^{-4}$ and using the model response function indicated in Fig. 4 to compute the model paradigm. Each row represents four selected image slices in one volunteer, and columns show approximately the same slice from four different volunteers. Areas of BOLD activity are indicated in light blue and dark blue for two experiments, and areas of SEEP activity are indicated in light red and dark red for two experiments. Where the BOLD and SEEP areas of activity overlap, the voxels are highlighted in yellow. The images are cropped to show only the right and left sensory and motor areas, for clarity.

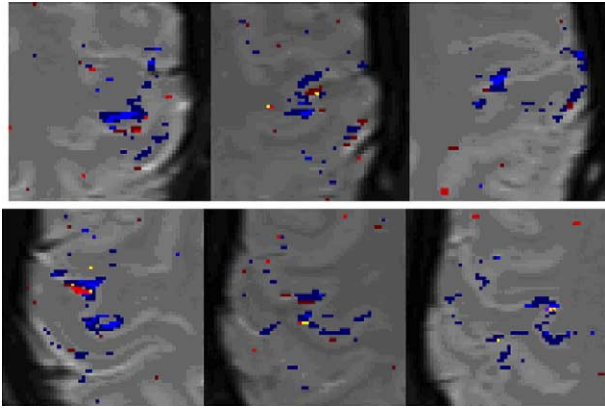


Fig. 3. Example of the detail of the areas of BOLD and SEEP response in one selected volunteer. The top row shows activity in three contiguous slices (superior to inferior going left to right) on the left side of the brain, and the bottom row shows the corresponding areas on the right side of the brain. Areas of BOLD activity are indicated in blue, and red indicates SEEP activity, with areas of overlap highlighted in yellow, as in Fig. 2.

Analyses based on the general-linear-model method described above in the Methods section were carried out in an iterative fashion, and so the optimal response functions, and optimal maps of activity, were obtained in parallel. Results of this method with a P -value threshold of $\leq 10^{-4}$ (corresponding to $T \geq 4.16$) also showed activity with both BOLD and SEEP with a high degree of localization to gray-matter regions in the sensory–motor cortex. The number of active voxels that were detected increased with the iterative process described above to

obtain the best estimate of the response functions for BOLD and SEEP. Representative activation maps from four of the eight subjects obtained with the general-linear-model analysis, the best response function and P values of $\leq 10^{-4}$ are shown in Fig. 2, with both areas of BOLD and SEEP contrast indicated on each figure. An example of these results from one subject is also shown in Fig. 3 with a greater degree of magnification to demonstrate the relative areas of BOLD and SEEP activity.

The response functions we measured were distinct for BOLD and SEEP contrast, but the results were consistent within and across the eight subjects. Using the definition of the BOLD hemodynamic response function from SPM2 (Statistical Parametric Mapping, Wellcome Department of Imaging Neuroscience, University College London) as a consistent means of describing the response, the parameters that varied included the time-to-peak response, the time-to-poststimulus undershoot and the relative magnitude of the poststimulus undershoot. The BOLD response function computed from the results of the present study has a time-to-peak response of 5 s, and time-to-poststimulus undershoot of 12 s. The relative magnitude of the poststimulus undershoot was 1/5 of the peak response. In comparison, the SEEP response function was observed to be 6 s to peak response, and the poststimulus response was observed to decay slowly. The poststimulus decay was best modelled by specifying 16 s to the peak poststimulus response, and a negative “undershoot” relative magnitude of $-1/6$. Plots of the average response functions calculated for the eight volunteers, and the best estimated

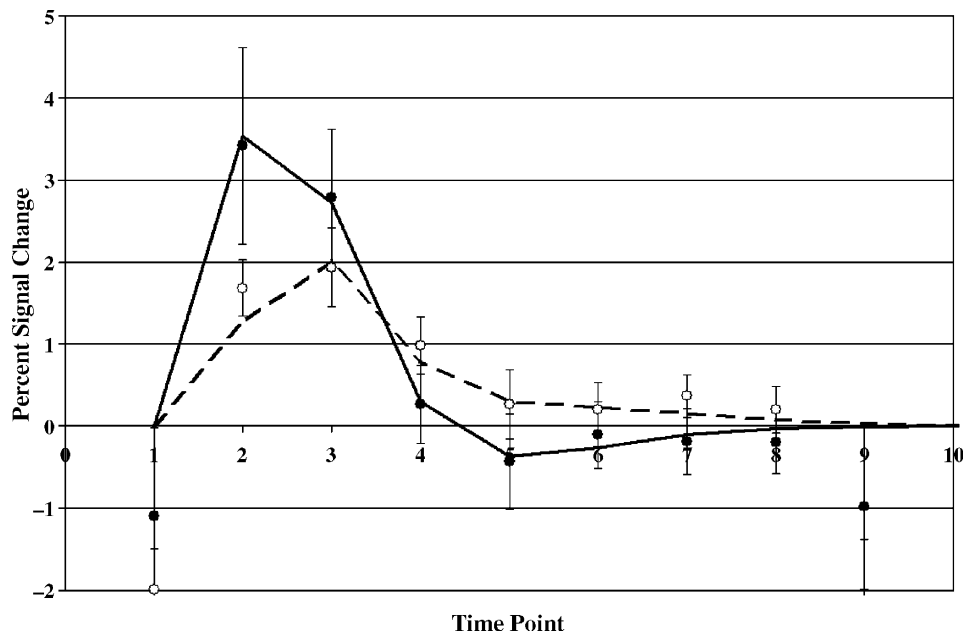


Fig. 4. Plots of the calculated response functions with BOLD and SEEP contrast at 1.5 T with high-resolution image data. The solid line represents the model BOLD response function, and the solid black dots indicate the measured response averaged over eight healthy volunteers. The dashed line represents the model SEEP response function, and the white dots indicate the averaged measured response. The error bars indicate the standard deviation of the measured response at each time point.

model functions, are shown in Fig. 4. These plots also show that the signal-intensity changes during the motor task averaged $3.4 \pm 1.2\%$ (mean \pm S.D.) with BOLD fMRI and $1.9 \pm 0.5\%$ with SEEP fMRI.

The proportion of active voxels identified within gray matter, white matter and CSF, with BOLD and SEEP contrast, were characterized based on segmented images of the three tissue types based on anatomical reference images with three different contrasts. However, the automated segmentation method used could not unambiguously identify all voxels, and so voxels containing a mixture of gray and white matter are identified as such. Active voxels with BOLD contrast were observed to be $60 \pm 6\%$ within gray matter, $13 \pm 3\%$ in a mix of gray and white matter, and $21 \pm 6\%$ in white matter. With SEEP contrast, $57 \pm 6\%$ of active voxels were observed within gray matter, $12 \pm 3\%$ in a mix of gray and white matter, and $24 \pm 5\%$ in white matter.

4. Discussion

Functional magnetic resonance imaging data acquired with proton density-weighted spin-echo imaging consistently demonstrated signal-intensity changes correlated with the motor-task paradigm and agreed with results obtained in previous studies at 0.2 and 3 T [2,3]. Analyses carried out using a nonlinear least squares method, with a basis set that includes either the calculated BOLD or SEEP response function, demonstrated voxels with signal changes that are significantly correlated to the model paradigm at $P \leq 10^{-4}$. This demonstrates that signal changes can be detected in proton density-weighted spin-echo fMRI data with a fairly high statistical threshold with an appropriate model response function. Active regions were confined to the bilateral sensory-motor areas and the supplementary motor areas, and were matched by areas of activity identified with conventional BOLD fMRI. Moreover, conjunction maps computed from duplicate experiments in each volunteer demonstrated that the same voxels were repeatedly observed to be active with both BOLD and SEEP contrast, as shown in the examples in Fig. 1. These maps therefore demonstrate that the results obtained with SEEP contrast are reproducible on a voxel-by-voxel basis.

The spatial distribution of activity observed in the present study demonstrates that the active voxels detected with SEEP contrast are in close proximity to those detected with BOLD contrast, but are immediately adjacent and not at the same locations, as demonstrated in Fig. 2. This is consistent with our previous study at 3 T [2] and indicates that SEEP and BOLD signal changes occur at different anatomical sites. As BOLD signal changes are known to occur in proximity with capillaries, venules and veins, SEEP signal changes can therefore be concluded to occur predominantly near capillaries, arterioles and arteries. This is consistent with the theory that the signal changes arise as a result of increased perfusion pressure, as pressure changes are expected to be larger in the less compliant vessels. Of the

active voxels detected in the brain, 69% to 73% were observed to be in voxels containing gray matter, or a mix of gray and white matter, and 21% to 24% were observed to be in white matter for BOLD and SEEP contrast, respectively, with no significant differences detected between the two. The greatest limitation of these measurements is expected to be the accuracy of the segmented image maps to define the tissue types within each voxel. Nonetheless, the observed consistency of the areas of SEEP activity with the neuroanatomy and areas of BOLD activity supports the conclusion that the SEEP signal changes are also related to neuronal activity.

The magnitude of signal intensity changes detected at 1.5 T in this study with SEEP contrast was $1.9 \pm 0.2\%$ (mean \pm S.E.M., $n=8$). This is in excellent agreement with previous studies which revealed signal changes of $1.9 \pm 0.3\%$ at 3 T and $2.1 \pm 0.2\%$ (right hand) and $2.3 \pm 0.1\%$ (left hand) at 0.2 T under similar conditions [2,3]. These values are not significantly different and further support our theory that the SEEP effect is field-independent and arises from a change in proton density. Each of these studies was carried out with different groups of healthy volunteers, and all demonstrated activity primarily in areas of the brain relevant to the hand motor task that was employed to elicit activity.

The magnitude of signal changes observed with BOLD contrast in the present study was $3.4 \pm 0.5\%$ (mean \pm S.E.M., $n=8$) with an echo time of 50 ms. This signal change corresponds to a ΔR_2^* value of -0.68 s^{-1} and is consistent with values reported in the literature [31]. The response function computed from data with BOLD contrast differed only slightly from the default hemodynamic response function used in SPM2. The shape of the response was as expected, but the duration was shorter. The default values in SPM2 employ a 6-s delay to the peak response, 16 s to the peak of the poststimulus undershoot and an undershoot ratio of 1/6 of the peak response. In this study, we observed 5 s to peak and 12 s to the peak of the undershoot, which had a magnitude of 1/5 of the peak. The response function for SEEP lagged the BOLD response with 6 s to the peak and a slower poststimulus decline which was modelled with a negative undershoot value of $-1/6$ of the peak response, as shown in Fig. 4. These values were computed from active voxels detected with a statistical threshold of $P \leq 10^{-4}$. Moreover, the response functions measured across the eight different volunteers were very consistent, for both BOLD and SEEP, as indicated by the error bars in Fig. 4. The distinct response functions identified for BOLD and SEEP, and the highly consistent SEEP response across different subjects, support the conclusion that the SEEP signal changes arise from different physiological processes than the BOLD effect.

Based on the magnitude of the BOLD signal changes observed with gradient-echo EPI in the current study, the BOLD contribution to our spin-echo data is estimated to be a signal change of less than 0.4%. This estimate is based on

the fact that the magnitude of the BOLD signal change has been shown to be at least 3.5 times larger in gradient-echo data than in spin-echo data at the same echo time [5,31]. Comparisons of the anatomical locations of SEEP and BOLD activity in this study, and previously at 3 T, have demonstrated that there is only slight overlap between the areas of activity, and so the average signal changes arising from SEEP and BOLD cannot be assumed to be cumulative [2]. Previous studies at 0.2 T have proven that SEEP signal changes cannot be attributed to residual BOLD effect, and this conclusion is supported by the current observations. Although the lines of k -space acquired with EPI have varying degrees of T_2^* -weighting, it is only the center of k -space that determines the weighting of the resulting image data, and with the symmetric spin echo employed in this study the center is T_2 -weighted. The varied weighting across lines of k -space influences the resulting image resolution but not the relaxation-time weighting [32]. The effect can be modelled by multiplying the k -space data by an exponential weighting function before reconstructing the image, and Fourier theory demonstrates that this is equivalent to convolving the reconstructed image with a smoothing filter with a Lorentzian profile (the Fourier transform of the exponential function). Hence the effect of the echo-planar sampling of k -space does not impose any inherent T_2^* weighting that could confound the comparison between BOLD and SEEP data. Moreover, the echo-planar k -space sampling employed in this study is expected to have had an identical effect on the resolution of our spin-echo and gradient-echo image data.

5. Conclusions

Functional magnetic resonance imaging based on a non-BOLD-contrast mechanism, which we have termed “SEEP”, has been demonstrated and characterized. Compared to the BOLD response function, the SEEP response function has a peak that lags by approximately 1 s, and a slower decay after stimulation is discontinued, with no poststimulus undershoot. The magnitude of the SEEP response has been consistently observed to be approximately 2%, independent of magnetic field strength, and areas of activity identified with SEEP are immediately adjacent to areas of BOLD signal changes with very little overlap. Areas of SEEP signal intensity changes have been shown to be detectable with a fairly stringent statistical threshold ($P \leq 10^{-4}$) and cannot be attributed to random effects or in-flow of fully relaxed blood, but can only be concluded to arise as a consequence of physiological changes related to neuronal activity. The SEEP effect is proposed to arise from a local change in fluid balance which may result from changes in perfusion pressure, production of extracellular fluid, cellular swelling and maintenance of ion and neurotransmitter concentrations at sites of neuronal activity. These mechanisms are consistent with known physiology. The existence of effects that can alter the MR signal intensity related to a

change in neuronal activity level, other than the BOLD effect, may be an expected result based on the myriad of known physiological changes that occur when neuronal firing rates increase. This is not to suggest that other methods should replace BOLD fMRI, but that alternative methods may provide supplementary information for neurophysiological studies and functional neuroimaging.

Acknowledgments

We are very grateful to Amanda Bergman for helpful input to this project. This work was undertaken, in part, thanks to funding from the Canada Research Chairs Program (P.W. Stroman).

References

- [1] Logothetis NK, Pauls J, Augath M, Trinath T, Oeltermann A. Neurophysiological investigation of the basis of the fMRI signal. *Nature* 2001;412(6843):150–7.
- [2] Stroman PW, Tomanek B, Krause V, Frankenstein UN, Malisza KL. Functional magnetic resonance imaging of the brain based on signal enhancement by extravascular protons (SEEP fMRI). *Magn Reson Med* 2003;49(3):433–9.
- [3] Stroman PW, Malisza KL, Onu M. Functional magnetic resonance imaging at 0.2 tesla. *Neuroimage* 2003;20:1210–4.
- [4] Stroman PW, Krause V, Malisza KL, Frankenstein UN, Tomanek B. Extravascular proton-density changes as a non-BOLD component of contrast in fMRI of the human spinal cord. *Magn Reson Med* 2002;48(1):122–7.
- [5] Stroman PW, Krause V, Frankenstein UN, Malisza KL, Tomanek B. Spin-echo versus gradient-echo fMRI with short echo times. *Magn Reson Imaging* 2001;19(6):827–31.
- [6] Wong KK, Ng MC, Hu Y, Luk DK, Ma QY, Yang ES. Functional MRI of the spinal cord at low field. Proceedings of the International Society for Magnetic Resonance in Medicine 12th Annual Meeting, Kyoto, Japan, May 15–21. 2004. p. 1534.
- [7] Jochimsen TH, Norris DG, Mildner T, Moller HE. Quantifying the intra- and extravascular contributions to spin-echo fMRI at 3 T. *Magn Reson Med* 2004;52(4):724–32.
- [8] Jochimsen TH, Norris DG, Moller HE. Is there a change in water proton density associated with functional magnetic resonance imaging? *Magn Reson Med* 2005;53(2):470–3.
- [9] Luh WM, Birn R, Bandettini PA. Proton-density increase measured by gradient-echo and spin-echo TE-stepping EPI during functional motor activation. Organization for Human Brain Mapping, New York, NY, June 18–22. 2003. p. 682.
- [10] Luh WM, Birn R, Bandettini PA. Echo relaxation imaging (ERI) demonstrates that activation induced spin-echo changes are not due to changes in T_2 . International Society for Magnetic Resonance in Medicine, 11th Scientific Meeting and Exhibition, Toronto, ON, July 10–16. 2003. p. 124.
- [11] Ng MC, Wong KK, Li G, Ma QY, Yang ES, Hu Y, et al. Verification of proton density change in spinal cord fMRI. Proceeding of the Fourth IASTED International Conference on Visualization, Imaging, and Image Processing, Marbella, Spain, September 6–8, 2004. p. 926.
- [12] Fitzgerald MJT, Folan-Curran J. Clinical neuroanatomy and related neuroscience. 4th ed. Toronto: WB Saunders; 2002 [50 pp].
- [13] Abbott NJ. Evidence for bulk flow of brain interstitial fluid: significance for physiology and pathology. *Neurochem Int* 2004; 45(4):545–52.
- [14] Fujita H, Meyer E, Reutens DC, Kuwabara H, Evans AC, Gjedde A. Cerebral [^{15}O] water clearance in humans determined by positron

- emission tomography: II. Vascular responses to vibrotactile stimulation. *J Cereb Blood Flow Metab* 1997;17(1):73–9.
- [15] Ohta S, Meyer E, Fujita H, Reutens DC, Evans A, Gjedde A. Cerebral [^{15}O]water clearance in humans determined by PET: I. Theory and normal values. *J Cereb Blood Flow Metab* 1996;16(5):765–80.
- [16] Ogawa S, Menon RS, Tank DW, Kim SG, Merkle H, Ellermann JM, et al. Functional brain mapping by blood oxygenation level-dependent contrast magnetic resonance imaging. A comparison of signal characteristics with a biophysical model. *Biophys J* 1993;64(3):803–12.
- [17] Ogawa S, Tank DW, Menon R, Ellermann JM, Kim SG, Merkle H, et al. Intrinsic signal changes accompanying sensory stimulation: functional brain mapping with magnetic resonance imaging. *Proc Natl Acad Sci U S A* 1992;89(13):5951–5.
- [18] Paulson OB, Newman EA. Does the release of potassium from astrocyte endfeet regulate cerebral blood flow? *Science* 1987;237(4817):896–8.
- [19] Andrew RD, MacVicar BA. Imaging cell volume changes and neuronal excitation in the hippocampal slice. *Neuroscience* 1994;62(2):371–83.
- [20] Nicholls JG, Martin AR, Wallace BG. Properties and functions of neuroglial cells. From neuron to brain. 3rd ed. Sunderland (Mass): Sinauer Associates; 1992. p. 146–83.
- [21] Amiry-Moghaddam M, Ottersen OP. The molecular basis of water transport in the brain. *Nat Rev Neurosci* 2003;4(12):991–1001.
- [22] Nedergaard M, Takano T, Hansen AJ. Beyond the role of glutamate as a neurotransmitter. *Nat Rev Neurosci* 2002;3(9):748–55.
- [23] Brodal P. The central nervous system, structure and function. 2nd ed. Oxford (NY): Oxford University Press; 1998 [20 p].
- [24] Sykova E, Vargova L, Kubinova S, Jendelova P, Chvatal A. The relationship between changes in intrinsic optical signals and cell swelling in rat spinal cord slices. *Neuroimage* 2003;18(2):214–30.
- [25] Sykova E. Diffusion properties of the brain in health and disease. *Neurochem Int* 2004;45(4):453–66.
- [26] Anderson TR, Andrew RD. Spreading depression: imaging and blockade in the rat neocortical brain slice. *J Neurophysiol* 2002;88(5):2713–25.
- [27] Friston KJ, Holmes AP, Poline JB, Grasby PJ, Williams SC, Frackowiak RS, et al. Analysis of fMRI time-series revisited. *Neuroimage* 1995;2(1):45–53.
- [28] Friston KJ, Holmes AP, Price CJ, Buchel C, Worsley KJ. Multi-subject fMRI studies and conjunction analyses. *Neuroimage* 1999;10(4):385–96.
- [29] Friston KJ, Jezzard P, Turner R. Analysis of functional MRI time-series. *Hum Brain Mapp* 1994;1:153–71.
- [30] Worsley KJ, Friston KJ. Analysis of fMRI time-series revisited—again. *Neuroimage* 1995;2(3):173–81.
- [31] Bandettini PA, Wong EC, Jesmanowicz A, Hinks RS, Hyde JS. Spin-echo and gradient-echo EPI of human brain activation using BOLD contrast: a comparative study at 1.5 T. *NMR Biomed* 1994;7(1–2):12–20.
- [32] Constable RT, Gore JC. The loss of small objects in variable TE imaging: implications for FSE, RARE, and EPI. *Magn Reson Med* 1992;28(1):9–24.